JPET Fast Forward. Published on September 10, 2015 as DOI: 10.1124/jpet.115.227223
This article has not been copyedited and formatted. The final version may differ from this version.

A Mechanistic PK/PD Model of Factor D Inhibition in Cynomolgus Monkeys by Lampalizumab for the Treatment of Geographic Atrophy

Kha N. Le, Leonid Gibiansky, Jeremy Good, Teresa Davancaze, Menno van Lookeren Campagne, Kelly M. Loyet, Alyssa Morimoto, Jin Jin, Lisa A. Damico-Beyer, William D. Hanley

Genentech Inc., South San Francisco, CA (K.N.L., J.G., T.D., M.v.L.C., K.M.L., A.M., J.J., L.A.D.-B., W.D.H.) and Quantpharm LLC., North Potomac, MD (L.G.)

Primary laboratory of origin: Covance

Downloaded from jpet.aspetjournals.org at ASPET Journals on April 17, 2024

JPET Fast Forward. Published on September 10, 2015 as DOI: 10.1124/jpet.115.227223
This article has not been copyedited and formatted. The final version may differ from this version.

JPET #227223

Running title (48/≤60 characters): TMDD Model of Lampalizumab in Cynomolgus Monkeys

Correspondence:

William Hanley

1 DNA Way, 46-3

South San Francisco, CA 94080

Ph: 650-467-8781

Fax: 650-472-5218

Email: Hanley.william@gene.com

Number of text pages: 14

Number of tables: 2

Number of figures: 6

Number of references: 28

Number of words in abstract: 250 words

Number of words in introduction: 616 words

Number of words in discussion: 1429 words

List of nonstandard abbreviations: ACP, alternative complement pathway; AMD, age-related macular degeneration; CFD, complement factor D; ELISA, enzyme-linked immunosorbent assay; Fab, antigen-binding fragment; GA, geographic atrophy; GLP, Good Laboratory Practice; HRP, horseradish peroxidase; ITV, intravitreal; mAb, monoclonal antibody; PD, pharmacodynamic; PK, pharmacokinetic; RPE, retinal pigment epithelium; RSE, relative standard error; TMB, tetramethylbenzidine; TMCL, target-mediated clearance; TMDD, target-mediated drug disposition.

Recommended section assignment: Drug Discovery and Translational Medicine

Downloaded from jpet.aspetjournals.org at ASPET Journals on April 17, 2024

JPET Fast Forward. Published on September 10, 2015 as DOI: 10.1124/jpet.115.227223
This article has not been copyedited and formatted. The final version may differ from this version.

Abstract (250/250 words)

Lampalizumab is an antigen-binding fragment of a humanized monoclonal antibody against complement factor D (CFD), a rate-limiting enzyme in the activation and amplification of the alternative complement pathway (ACP), that is in phase III clinical trials for the treatment of geographic atrophy. Understanding of the pharmacokinetics, pharmacodynamics, and biodistribution of lampalizumab following intravitreal administration in the ocular compartments and systemic circulation is limited, but crucial for selecting doses that provide optimal efficacy and safety. Here we sought to construct a semi-mechanistic and integrated ocular-systemic pharmacokinetic-pharmacodynamic model of lampalizumab in the cynomolgus monkey to provide a quantitative understanding of the ocular and systemic disposition of lampalizumab and CFD inhibition. The model takes into account target-mediated drug disposition, target turnover, and drug distribution across ocular tissues and systemic circulation. Following intravitreal administration, lampalizumab achieves rapid equilibration across ocular tissues. Lampalizumab ocular elimination is relatively slow with a $\tau_{1/2}$ of approximately 3 days, while systemic elimination is rapid with a $\tau_{1/2}$ of 0.8 hours. Target-independent linear clearance is predominant in the eye, whereas target-mediated clearance is predominant in the systemic circulation. Systemic CFD synthesis was estimated to be high (7.8 mg/day); however, the amount of CFD entering the eye due to influx from the systemic circulation was small (<10%) compared with the lampalizumab dose and is thus expected to have an insignificant impact on the clinical dose-regimen decision. Our findings support the clinical use of intravitreal lampalizumab to achieve significant ocular ACP inhibition while maintaining low systemic exposure and minimal systemic ACP inhibition.

Downloaded from jpet.aspetjournals.org at ASPET Journals on April 17, 2024

JPET Fast Forward. Published on September 10, 2015 as DOI: 10.1124/jpet.115.227223
This article has not been copyedited and formatted. The final version may differ from this version.

Introduction (616/750)

Geographic atrophy (GA) is an advanced stage of age-related macular degeneration (AMD) and is characterized by the loss of retinal photoreceptors, retinal pigment epithelium (RPE), and choriocapillaris. Vision loss in GA is progressive, and approximately 20% of legal cases of blindness in North America are due to GA (Holz et al., 2014; van Lookeren Campagne et al., 2014). Worldwide, there are more than 5 million people with GA (Sunness et al., 1997; Wong et al., 2014). Despite the increasing prevalence of GA, it currently remains a largely unmet clinical need as no approved therapy is available (Girmens et al., 2012). The pathogenesis of AMD is not well understood; however, genetic and environmental factors appear to contribute to the disease process (de Jong, 2006). The alternative complement pathway has been implicated in AMD by both human genetics and histopathology. Genetic epidemiology studies have demonstrated that polymorphisms in alternative complement pathway-associated genes have strong correlations with the risk of developing AMD (Fritsche et al., 2013). In addition, activated components of the alternative complement pathway have been found in drusen (lipoproteinous depositions in the space between the RPE and Bruch's membrane), which are a hallmark of AMD. These findings suggest that the alternative complement pathway may be an important mediator of AMD.

Lampalizumab (Genentech, Inc., South San Francisco, CA) is the antigen-binding fragment (Fab) of a humanized monoclonal antibody (mAb) that inhibits complement factor D (CFD), which is the rate-limiting enzyme in the activation and amplification of the alternative complement pathway (Katschke et al., 2012). Lampalizumab intravitreal (ITV) injection is under evaluation for the treatment of GA. The phase Ia (NCT00973011) (Do et al., 2014) and the Mahalo phase Ib/II clinical trials (NCT01229215) have been completed. Lampalizumab was shown to have an acceptable safety profile when administered at 10 mg per eye (Do et al., 2014). Two phase III, double-masked, multicenter, randomized, sham injection-controlled studies (NCT02247479 [Chroma] and NCT02247531 [Spectri]) are under way.

Retinal diseases such as AMD are difficult to treat, partly because the anatomy of the eye makes drug delivery to its posterior segment challenging (Kang-Mieler et al., 2014). Intravitreal delivery is the most

Downloaded from jpet.aspetjournals.org at ASPET Journals on April 17, 2024

JPET Fast Forward. Published on September 10, 2015 as DOI: 10.1124/jpet.115.227223
This article has not been copyedited and formatted. The final version may differ from this version.

direct drug delivery method to treat retinal diseases. Understanding of the pharmacokinetics (PK), pharmacodynamics (PD), and biodistribution of such an ITV-administered drug and its target in the ocular compartments and systemic circulation is limited, but crucial, to allow for optimal dosing and ensure efficacy and safety. PK/PD modeling provides a useful quantitative framework to evaluate ocular and systemic drug disposition as it accounts for all processes governing the PK characteristics (such as antigen binding, distribution, and clearance processes) and corresponding PD effects (Agoram et al., 2007; Luu et al., 2013; Schuck et al., 2015; Van Der Graaf and Gabrielsson, 2009). A target-mediated drug disposition (TMDD) model is critical in explaining the PK and PD of many biologics for which the high antibody-target binding affinity as well as the antibody and target levels can directly influence the PK of the antibody (Mager and Jusko, 2001). Lampalizumab was shown to bind CFD in both human and cynomolgus monkey (*Macaca fascicularis*) species with high affinity (Loyet et al., 2014). Cynomolgus monkeys were shown to be a relevant preclinical model for evaluating PK/PD of lampalizumab (Katschke et al., 2012; Loyet et al., 2014). A single ITV dose-escalation study, a 2-week single-dose ITV toxicity study, and a PK study of intravenous (IV) or ITV injections of lampalizumab were performed in cynomolgus monkeys. The objective of this analysis is to develop a semi-mechanistic and integrated ocular-systemic PK/PD model of lampalizumab in cynomolgus monkey to provide a quantitative understanding of the disposition of lampalizumab and inhibition of CFD in both ocular tissues and systemic circulation following ITV administration of lampalizumab.

Downloaded from jpet.aspetjournals.org at ASPET Journals on April 17, 2024

JPET Fast Forward. Published on September 10, 2015 as DOI: 10.1124/jpet.115.227223
This article has not been copyedited and formatted. The final version may differ from this version.

Methods

Lampalizumab Pharmacokinetic and Pharmacodynamic Studies

Table 1 summarizes the designs of the three studies included in this analysis. These preclinical studies were conducted in both male and female cynomologus monkeys at Covance (Madison, WI). The studies were approved by the Covance Institutional Animal Care and Use Committee. The studies were conducted in compliance with United States Food and Drug Administration regulations for Good Laboratory Practice (GLP) for Nonclinical Laboratory Studies (21 CFR Part 58) and the US Department of Agriculture Animal Welfare Act Regulations (9 CFR 3), *Guide for the Care and Use of Laboratory Animals*. Lampalizumab was administered via a single IV or ITV injection at the indicated dosage. For IV administration, lampalizumab was administered as a single bolus dose into the saphenous vein. For ITV administration, lampalizumab was administered as a single injection into both eyes.

Baseline (pre-dose) and post-dose blood samples for PK analysis were collected from each animal via a femoral vein at time points indicated in Table 1. Blood samples were collected in serum separator tubes without anticoagulant, allowed to clot at ambient temperature for at least 20 minutes, and then centrifuged in a refrigerated centrifuge set to 2–8°C. The serum was harvested within 20 minutes of centrifugation and stored between -60°C and -80°C before PK analysis. Following euthanasia, vitreous humor, aqueous humor, and retinal tissue were collected from both eyes. Retinal tissue collected included neuroretina and RPE/choroid, and excluded sclera. Additionally, a strip of retinal tissue including the disc, macula, and peripheral retina was collected. Retinal tissue samples were weighed and recorded. All ocular matrix samples were stored at -80°C before analysis.

Analysis of Lampalizumab and CFD

Lampalizumab in Cynomolgus Monkey Serum

The concentration of lampalizumab in male and female cynomolgus monkey serum was measured by enzyme-linked immunosorbent assay (ELISA). A mouse mAb to lampalizumab (clone 7470; Genentech, Inc., South San Francisco, CA) was adsorbed to the surface of microtiter plates overnight at 2–8˚C to capture total lampalizumab (bound and unbound to CFD). After a 2-hour incubation, goat anti-human IgG-

Downloaded from jpet.aspetjournals.org at ASPET Journals on April 17, 2024

JPET Fast Forward. Published on September 10, 2015 as DOI: 10.1124/jpet.115.227223
This article has not been copyedited and formatted. The final version may differ from this version.

HRP (Bethyl, Montgomery, TX), which detects lampalizumab in the presence or absence of CFD, was added for 1 hour. TMB substrate (40 mM TMB, 8 mM tetrabutylammonium borohydride, in N,N′-dimethylacetamide) was subsequently added and the reaction was stopped with 1M phosphoric acid after optimal color development. Absorbance was measured photometrically at 450 nm and referenced to 650 nm. The standard curve ranged from 2.5 to 320 ng/ml. The minimum quantifiable concentration of total lampalizumab in cynomolgus monkey serum was 10 ng/ml.

Lampalizumab in Cynomolgus Monkey Aqueous Humor, Vitreous Humor, and Retinal Tissue

The concentration of lampalizumab in cynomolgus monkey aqueous humor, vitreous humor, and retinal tissue was measured by ELISA as described above. The standard curve ranged from 12.5 to 1600 ng/ml. Retinal tissue samples were homogenized and the homogenate was analyzed in the ELISA. Retinal tissue results were normalized by tissue weight. The minimum quantifiable concentration of total lampalizumab in cynomolgus monkey aqueous humor, vitreous humor, and retinal tissue was 26.3 ng/ml.

Factor D in Cynomolgus Monkey Serum

The concentration of CFD in cynomolgus monkey serum was measured using an ELISA. A mouse mAb specific to CFD (clone 4676; Genentech, Inc., South San Francisco, CA) was adsorbed to the surface of microtiter plates overnight at 2–8˚C to capture total CFD (bound and unbound to lampalizumab). Lampalizumab was then added to samples to saturate CFD-binding sites. After a 2-hour incubation, biotin-labeled mAb 7470 was added for 1 hour. Streptavidin-HRP (Thermo Scientific, Waltham, MA) was added for 1 hour. Substrate incubation and reading of the plate were performed as described for the lampalizumab serum method. The standard curve ranged from 3.9 to 500 ng/ml. The minimum quantifiable concentration of total CFD in cynomolgus monkey serum was 5 ng/ml.

Factor D in Cynomolgus Monkey Aqueous and Vitreous Humor

The concentration of CFD in cynomolgus monkey aqueous humor and vitreous humor was measured by ELISA as described for the CFD serum method with the following modifications. The standard curve

Downloaded from jpet.aspetjournals.org at ASPET Journals on April 17, 2024

JPET Fast Forward. Published on September 10, 2015 as DOI: 10.1124/jpet.115.227223
This article has not been copyedited and formatted. The final version may differ from this version.

ranged from 0.8 to 100 ng/ml. The minimum quantifiable concentration of total CFD in cynomolgus monkey aqueous and vitreous humor was 2 ng/ml.

Target-Mediated Drug Disposition Model

All ocular and serum (following IV and ITV) data were simultaneously analyzed using a TMDD model that incorporates the binding equilibrium and in vivo turnover rates of free CFD, lampalizumab, and drug-target (lampalizumab-CFD) complex as depicted by Figure 1. NONMEM software (version 7.2, ICON Development Solutions) was used to perform all model estimation and simulation.

A quasi-steady state approximation (Gibiansky et al., 2008) of the TMDD model described the total vitreous lampalizumab concentrations (unbound and bound to CFD) and total vitreous CFD concentrations (unbound and bound to lampalizumab). Equations that describe the final model are shown below:

$$(1)\ \frac{dA_{VITR}}{dt} = -k_{out}.\,C_{vu}.\,V_{VITR} - k_{outC}\,\frac{R_{VITR}.C_{vu}.V_{VITR}}{K_{ss}+C_{vu}} + k_{inC}\,\frac{R_{SER}.C_{su}.V_C}{K_{ss}+C_{su}}$$

$$(2)\ \frac{dR_{VITR}}{dt} = k_{SV}.\,\frac{R_{SER}.K_{ss}.V_C}{(K_{ss}+C_{su}).V_{VITR}} - k_{outT}.\,\frac{R_{VITR}.K_{ss}}{K_{ss}+C_{vu}} - k_{outC}.\,\frac{R_{VITR}.C_{vu}.V_{VITR}}{K_{ss}+C_{vu}} + k_{inC}\,\frac{R_{SER}.C_{su}.V_C}{(K_{ss}+C_{su}).V_{VITR}}$$

$$(3)\ \frac{dA_{SER}}{dt} =$$

$$2\left(k_{out}.\,C_{vu}.\,V_{VITR} + k_{outC}\,\frac{R_{VITR}.C_{vu}.V_{VITR}}{K_{ss}+C_{vu}}\right) - k.\,C_{su}.\,V_c - k_{inT}.\,\frac{R_{SER}.C_{su}}{K_{ss}+C_{su}}.\,V_c - 2.\,k_{inC}\,\frac{R_{SER}.C_{su}.V_C}{K_{ss}+C_{su}} -$$

$$k_{12}.\,A_{SER} + k_{21}.\,A_{PER}$$

$$(4)\ \frac{dR_{SER}}{dt} = k_{syn} - k_{deg}.\,\frac{R_{SER}.K_{ss}}{K_{ss}+C_{su}} - k_{inT}.\,\frac{R_{SER}.C_{su}}{K_{ss}+C_{su}} - 2.\,k_{SV}.\,\frac{R_{SER}.K_{ss}}{K_{ss}+C_{su}}$$

$$+2.\,k_{outC}\,\frac{R_{VITR}.C_{vu}.V_{VITR}}{(K_{ss}+C_{vu}).V_C} + 2.\,k_{outT}.\,\frac{R_{VITR}.K_{ss}.V_{VITR}}{(K_{ss}+C_{vu}).V_C} - 2.\,k_{inC}\,\frac{R_{SER}.C_{su}}{K_{ss}+C_{su}} - k_{12T}.\,R_{SER} + k_{21T}.\,R_{PER}$$

$$(5)\ \frac{dA_{PER}}{dt} = k_{12}.\,A_{SER} - k_{21}.\,A_{PER,}$$

$$(6)\ \frac{dR_{PER}}{dt} = k_{12T}.\,R_{SER} - k_{21T}.\,R_{PER}$$

Downloaded from jpet.aspetjournals.org at ASPET Journals on April 17, 2024

JPET Fast Forward. Published on September 10, 2015 as DOI: 10.1124/jpet.115.227223
This article has not been copyedited and formatted. The final version may differ from this version.

$$(7)\ C_{vu} = \frac{1}{2}\left[(C_{VITR} - R_{VITR} - K_{ss}) + \sqrt{(C_{VITR} - R_{VITR} - K_{ss})^2 + 4.K_{ss}.C_{VITR}}\right],$$

$$(8)\ C_{su} = \frac{1}{2}\left[(C_{SER} - R_{SER} - K_{ss}) + \sqrt{(C_{SER} - R_{SER} - K_{ss})^2 + 4.K_{ss}.C_{SER}}\right]$$

$$(9)\ C_{AQ\_tot} = \frac{C_{VITR}}{\lambda_{VA}}$$

$$(10)\ R_{AQ} = \frac{R_{VITR}}{\lambda_{TVA}}$$

$$(11)\ C_{RET\_tot} = \frac{C_{VITR}}{\lambda_{VR}}$$

$$(12)\ C_{VITR} = \frac{A_{VITR}}{V_{VITR}}$$

$$(13)\ C_{SER} = \frac{A_{SER}}{V_C}$$

Here, equations 1, 2, 3, and 4 describe the kinetics of total lampalizumab amount in vitreous (A_{VITR}), total CFD concentration in vitreous (R_{VITR}), total lampalizumab amount in serum (A_{SER}), and total CFD concentration in serum (R_{SER}), respectively. Equations 5 and 6 describe the kinetics of the peripheral compartments for lampalizumab and CFD, respectively. Equations 7 and 8 describe the quasi-steady state approximation for the relationship between unbound lampalizumab concentrations in vitreous and serum (C_{vu} *and* C_{su}), total lampalizumab concentrations in vitreous and serum (C_{VITR} *and* C_{SER}), and total CFD concentration in vitreous and serum (R_{VITR} *and* R_{SER}), respectively. Equation 9 describes the relationship between aqueous (C_{AQ_tot}) and vitreous (C_{VITR}) total lampalizumab concentrations and the vitreous-aqueous lampalizumab partition coefficient (λ_{AQ}). Equation 10 describes the relationship between total CFD levels in aqueous (R_{AQ}), vitreous (R_{VITR}), and the vitreous-aqueous partition coefficient of total CFD (λ_{TAQ}). Equation 11 describes the relationship between retina (C_{RET_tot}) and vitreous (C_{VITR}) total lampalizumab concentrations and the vitreous-retina lampalizumab partition coefficient (λ_{VR}). The actual transfer rates for complex, free drug, and free target may be different. However, as there are not sufficient data to build a more complex model, we simplified the peripheral distribution process by using only two rate constants (k_{12} and k_{21}) for the drug rates and one rate constant (k_{12T}=k_{21T}) for the target rate. k_{12T} was assumed to be the same as k_{21T}. These are empirical parameters to improve the model goodness of fit of the IV arms.

Downloaded from jpet.aspetjournals.org at ASPET Journals on April 17, 2024

JPET Fast Forward. Published on September 10, 2015 as DOI: 10.1124/jpet.115.227223
This article has not been copyedited and formatted. The final version may differ from this version.

V_{VITR} and V_C are the vitreous and serum volumes, respectively; R_{AQ} is the total CFD concentration in aqueous; k_{out}, k_{outT}, and k_{outC} denote the ocular elimination rate constants of the unbound lampalizumab, free CFD, and lampalizumab-CFD complex, respectively; k_{outT} was fixed to a value of 0.3 day-1 based on the vitreous half-life of radioactively labeled factor D following ITV administration (unpublished in-house data). k, k_{deg}, and k_{inT} denote the systemic elimination rate constants of the unbound lampalizumab, free CFD, and lampalizumab-CFD complex, respectively. k_{syn} is the zero-order production rate constant of CFD in vitreous; k is the first-order clearance rate constant of lampalizumab in serum; k_{inC} is the first-order rate constant of lampalizumab-CFD complex from serum to vitreous, and was assumed to be negligible because the concentration of the complex is higher in the ocular environment following ITV administration; k_{SV} is the first-order rate constant of free CFD from serum to vitreous; and K_{SS} is the quasi-steady-state constant of lampalizumab binding to CFD. K_{SS} was fixed to the in vitro parameter of 11.7 pM (Loyet et al., 2014). F1 denotes the fraction of drug that enters the vitreous directly following ITV administration, and the remaining fraction (1-F1) was assumed to leak to the serum by fast absorption, presumably from the microcirculation.

Naïve-pool approach was used to model the data. The residual error model for the observations was best described by a proportional error model, and the proportional residual errors were assumed to be independent and normally distributed with zero means.

Model Simulations

A series of model simulations were performed using the estimated model parameters to examine the behavior of drug and target in ocular tissue and serum as a function of time and dose level to provide a better understanding of the PK/PD of lampalizumab. The fraction of drug eliminated via linear clearance or target-mediated clearance at time *t* are defined by equations 12 and 13, respectively, in the eye, and equations 14 and 15, respectively, in the serum. The time course of total target flux from systemic-to-ocular (R_{in}) was simulated (Equation 16) to understand the relative total target influx from systemic circulation to ocular tissues. All simulations were performed using NONMEM software.

Downloaded from jpet.aspetjournals.org at ASPET Journals on April 17, 2024

JPET Fast Forward. Published on September 10, 2015 as DOI: 10.1124/jpet.115.227223
This article has not been copyedited and formatted. The final version may differ from this version.

$$(12)\ f_{OcularLCL}(t) = \frac{\int_0^t k_{out}.C_{vu}.V_{VITR}.dt}{\int_0^t k_{out}.C_{vu}.V_{VITR}.dt + \int_0^t k_{outC}\frac{R_{VITR}.C_{vu}.V_{VITR}}{K_{ss}+C_{vu}}.dt}$$

$$(13)\ f_{OcularTMCL}(t) = 1 - f_{OcularLCL}(t)$$

$$(14) f_{SerumLCL}(t) = \frac{\int_0^t k_{inC}.C_{su}.V_C.dt}{\int_0^t k_{inC}.C_{su}.V_C.dt + \int_0^t \left(k_{inT}.\frac{R_{SER}.C_{su}}{K_{ss}+C_{su}}.V_C + 2.k_{inC}\frac{R_{SER}.C_{su}.V_C}{K_{ss}+C_{su}}\right).dt}$$

$$(15) f_{SerumTMCL}(t) = 1 - f_{SerumLCL}(t)$$

$$(16)\ R_{in}(t) = V_C.\int_0^t (k_{SV}.\frac{R_{SER}.K_{ss}}{K_{ss}+C_{su}} + k_{inC}\frac{R_{SER}.C_{su}}{(K_{ss}+C_{su})}).\ dt$$

Results

Ocular and Systemic Lampalizumab and CFD Concentration-Time Profiles Are Well Described by a TMDD Model

All available lampalizumab and CFD data (**Table 1**) in ocular tissues and serum were combined and fit using a TMDD model (**Figure 1**) with a single set of parameters. The observed concentration-time profiles of lampalizumab and total CFD in serum following IV and ITV administration were well described by the proposed combined ocular-serum PK/PD model. The model-predicted time courses of both lampalizumab and total CFD were in good agreement with the observed data at different dose levels in both serum (**Figures 2A and 2B**) and ocular (**Figures 2C, 2D, and 2E**) compartments. All model parameters were estimated with good precision with relative standard errors below 24%, except for the CFD distribution rate constant (53.8%) (**Table 2**).

The estimated ocular elimination half-life of lampalizumab was 2.9 days (k_{out} = 0.2 day^{-1}, relative standard error (RSE) = 2.1%) and was markedly longer than the systemic elimination half-life of 0.8 hours (k = 21.3 day^{-1}, RSE = 6.6%). Volumes of distribution of lampalizumab in the vitreous humor and serum were 2.2 and 127 ml (~32-64 ml/kg for 2–4 kg body weight in this study), respectively. These values are in broad agreement with the literature values for vitreous humor volume (Struble et al., 2014) and antibody volume

Downloaded from jpet.aspetjournals.org at ASPET Journals on April 17, 2024

JPET Fast Forward. Published on September 10, 2015 as DOI: 10.1124/jpet.115.227223
This article has not been copyedited and formatted. The final version may differ from this version.

distribution (Deng et al., 2011) in the cynomolgus monkey. For CFD, the elimination half-life from serum was estimated to be 0.2 hours (k_{deg} = 96.0 day^{-1}, RSE = 10.1%) and the synthesis rate was 2.6 nmol/ml/day or 7.8 mg/day. The elimination half-lives of lampalizumab-CFD complex from vitreous and serum were 0.9 days (k_{outC} = 0.7 day^{-1}, RSE = 16.9%) and 0.2 days (k_{int} = 4.2 day^{-1}, RSE = 5.6%), respectively.

Distribution Across Ocular Tissues Achieved Quick Equilibrium

Lampalizumab concentrations were determined in vitreous humor, aqueous humor, and the retina to help elucidate the pharmacokinetics within ocular tissues. Elimination rates of lampalizumab in the vitreous humor, aqueous humor, and retina were similar (half-life = 2.9 days). Maximum tissue concentrations in the vitreous, aqueous, and retina were observed at the first observed data point of 10 hours, which was shorter than the ocular elimination half-life of 2.9 days, suggesting that ocular tissue distribution achieved equilibrium relatively quickly. This was further supported by the evidence that aqueous humor, vitreous humor, and retina exposures can be related by a constant partition coefficient. The lampalizumab vitreous-aqueous partition coefficient was estimated to be 4.4 (RSE = 12.1%), and the vitreous-retina partition coefficient was 7.3 (RSE = 15.3%). Similarly, the partition coefficient of CFD between vitreous and aqueous was 0.5 (RSE = 23.5%).

Lampalizumab Administration Achieved High Ocular Target Occupancy With Transient Systemic CFD Inhibition

Ocular tissue concentrations of both lampalizumab and total CFD were determined in order to elucidate ocular pharmacokinetics and target occupancy with ITV administration of lampalizumab. Ocular lampalizumab levels in both vitreous and aqueous humor were well above the total CFD level (at least 10x higher) over the 16 days of the study (**Figures 2C and 2D**). Simulation of 1–10 mg of lampalizumab per eye showed that the vitreous total drug level exists as predominantly free drug and that the total target level exists as predominantly drug-target complex for the first 30–40 days following dosing (**Figure 3A**). The free target level is predicted to be well below (3–6 orders of magnitude below) the baseline

Downloaded from jpet.aspetjournals.org at ASPET Journals on April 17, 2024

JPET Fast Forward. Published on September 10, 2015 as DOI: 10.1124/jpet.115.227223
This article has not been copyedited and formatted. The final version may differ from this version.

target level over this period of time. In addition, ocular lampalizumab clearance was predominantly through linear clearance mechanism (more than ~99% of total clearance) with minimal target-mediated clearance over a simulated dose range of 0.1–50 mg/eye (**Figure 3B**).

The time courses of systemic lampalizumab and total CFD concentrations were quantified to assess the systemic pharmacokinetics of lampalizumab following ITV administration and potential systemic inhibition of CFD.

Systemic pharmacokinetics of lampalizumab exhibited flip-flop kinetics, a phenomenon in which systemic lampalizumab pharmacokinetics were limited by the ocular-to-serum absorption rate, and the serum terminal elimination rate in this case was reflective of the ocular-to-serum absorption rate (**Figures 2A and 2B**). In addition, systemic elimination following IV administration ($k = 21.3\ day^{-1}$) is substantially faster than that following ITV administration ($k_{out} = 0.2\ day^{-1}$) (**Table 2**). As a result of this rapid systemic clearance, the systemic lampalizumab level in the serum was low, with concentrations below the total CFD level for most of the 24 days of the study (**Figure 2B**). Simulation of 1–10 mg of lampalizumab per eye showed that the serum total drug level existed as predominantly drug-CFD complex up to 60 days following dosing (**Figure 4A**). The free target level only dropped transiently, with nadir at 2 and 19% below baseline for 1 and 10 mg, respectively, and recovered back to baseline target level within 10 days following dosing. In addition, systemic lampalizumab clearance was predominantly through the target-mediated clearance mechanism (more than 90% of total clearance) over a large dose range (0.1–50 mg/eye) (**Figure 4B**).

Target occupancy in the vitreous and serum was simulated using the TMDD model. Free CFD level in the vitreous dropped substantially upon ITV lampalizumab dosing, and maximum vitreous CFD inhibition occurred quickly (within 1 day following ITV dosing). More than 95% target occupancy was maintained for 34 and 44 days following a single ITV dose of 1 and 10 mg/eye, respectively (**Figures 5**). Systemic CFD inhibition was transient, with target occupancy in the serum reaching maximum target occupancy at 41

Downloaded from jpet.aspetjournals.org at ASPET Journals on April 17, 2024

JPET Fast Forward. Published on September 10, 2015 as DOI: 10.1124/jpet.115.227223
This article has not been copyedited and formatted. The final version may differ from this version.

and 89% for 1 and 10 mg per eye, respectively, within day 1 and decreasing approximately linearly over time. Recovery back to ~10% occupancy was at 8 and 17 days after dosing (**Figure 5**). Despite the moderate systemic target occupancy, the serum lampalizumab molar concentrations for the 1- or 10-mg dose groups either did not or only transiently exceeded the molar concentrations of CFD; this molar excess of lamaplizumab was shown to be necessary for systemic alternative complement pathway inhibition based on the ACP hemolytic activity (AH50) assay (Loyet et al., 2014).

Ocular Influx of CFD Following Intravitreal Lampalizumab Dosing

To study the extent of systemic-to-ocular influx of CFD, we examined the cumulative ocular influx over time as a function of dose using model simulations. Despite the high CFD synthesis in the serum (2.6 nmol/ml/day), the serum-to-ocular transfer rate constant of CFD was estimated to be small (3×10^{-4} day^{-1}) (**Table 2**). As a result, the cumulative ocular influx of CFD at 30 days following ITV dosing was small compared with total administered drug amount, at less than 10% and less than 1% of the 1- and 10-mg dose per eye, respectively (**Figure 6**).

Discussion (1429/1500)

Target-mediated drug disposition, whereby the pharmacokinetics of a drug are significantly altered by the process of binding to its biological target, was shown to be an important mechanism affecting the PK and PD of many biologics (Mager, 2006; Mager and Jusko, 2001). Understanding the TMDD of an investigative drug provides the understanding of drug levels and target occupancy at various tissue sites, and is ultimately an important tool in selecting the right dose level and regimen for therapeutic biologics. This is especially important for ocular-targeted biologics for which the target levels and turnover rates in the eye and the systemic circulation can be very different, such as those for CFD, which has a systemic synthesis rate estimated at 1.33 mg/kg per day compared to relatively few neural retina CFD transcripts and average systemic concentration of 42 nM, ~2.5 times higher than in post-mortem human vitreous humor (Anderson et al., 2010; Barnum et al., 1984; Loyet et al., 2012; Pascual et al., 1988). In this analysis, we sought to construct a semi-mechanistic PK/PD model of lampalizumab in both ocular tissues

Downloaded from jpet.aspetjournals.org at ASPET Journals on April 17, 2024

JPET Fast Forward. Published on September 10, 2015 as DOI: 10.1124/jpet.115.227223
This article has not been copyedited and formatted. The final version may differ from this version.

and serum in healthy cynolmogus monkeys. The intensive and invasive tissue sampling in the monkey model enables a mechanistic and integrated understanding of the interplay of the ocular and systemic PK/PD of lampalizumab. The results from this analysis provide a better understanding of the lampalizumab PK/PD and the constructed PK/PD model provides an important tool to predict and optimize future studies of lampalizumab for the treatment of geographic atrophy. For the purpose of extrapolating to humans, it should be noted that previous studies have shown plasma, but not vitreous humor, levels of CFD were significantly elevated in AMD patients compared to control cases (Hecker et al., 2010; Loyet et al., 2012; Scholl et al., 2008; Stanton et al., 2011).

The serum and ocular lampalizumab and CFD concentration time courses following a large range of both IV and ITV doses (**Table 1**) were well described (**Figure 2**) by a TMDD model that takes into account target binding, distribution, vitreous-aqueous and vitreous-retina partitioning, target turnover, and diffusion-driven transport processes across different ocular and serum compartments (**Figure 1**). Following ITV administration, lampalizumab is distributed to the aqueous and retina relatively quickly, within the first 45 minutes following dosing. Lampalizumab partitions relatively similarly between vitreous and aqueous (λ_{VR} = 4.4) and between vitreous and retina (λ_{VR} = 7.3). The ocular elimination half-life of lampalizumab in cynomologus monkeys was estimated to be approximately 3 days and was significantly longer than the systemic elimination half-life of 0.8 hours. A similar difference between ocular and systemic half-life was noted in a TMDD model of lampalizumab in humans (Le et al., 2015) in which the vitreous half-life was 5.9 days compared with a systemic half-life of 9 hours. The shorter ocular half-life in monkeys (3 days) compared to humans (7-9 days) was also reported for ranibizumab (Gaudreault et al., 2005; Krohne et al., 2012; Xu et al., 2013). Similar to the clinical results, lampalizumab in the cynomolgus monkey also exhibits flip-flop pharmacokinetics, a phenomenon in which the rate of drug egressing out of the vitreous is much slower than the rate of drug cleared from the systemic circulation. This phenomenon is also similar to that exhibited by ITV ranibizumab, a Fab (Xu et al., 2013), and ITV pegaptanib, a pegylated aptamer (Macugen package insert, 2011) , and helps to maintain low systemic exposure and minimize any potential systemic safety issues. There have been limited literature on comparison of ocular PK/PD properties for full length antibodies vs. Fab's. However, our results suggested that there appears

Downloaded from jpet.aspetjournals.org at ASPET Journals on April 17, 2024

JPET Fast Forward. Published on September 10, 2015 as DOI: 10.1124/jpet.115.227223
This article has not been copyedited and formatted. The final version may differ from this version.

to be no gain in half-life with higher molecular weight when comparing the ocular half-life of the free lampalizumab, free CFD and the lampalizumab-CFD complex (MW range from 24-72kD). The relationship between ocular half-life and molecular size is unknown beyond this range. However, literature on ITV administration of anti-VEGF therapy suggested that half-life of ranibizumab (7-9 days) (Krohne et al., 2012; Xu et al., 2013) was only slightly shorter than that for bevacizumab (9.8 days) (Krohne et al., 2012) in humans. Notably, the quasi-steady state equilibrium constant K_{ss} was fixed to the in vitro measured value of dissociation equilibrium constant (K_D) of 11.7 pM (Loyet et al., 2014), and was able to describe the data quite well. As quasi-equilibrium approximation is a special case of the quasi-steady state approximation (Gibiansky et al., 2008), and the in vitro and in vivo agreement of the parameters K_D and K_{ss} confirms the assumption that the internalization rate constant is much smaller than the dissociation rate constant.

In the cynolmolgus monkeys, ITV lampalizumab achieves near-complete target occupancy in the vitreous (**Figure 5A**). This is evidenced by the dramatically higher observed ocular lampalizumab concentrations compared with total ocular CFD levels (**Figure 2C-D**), and the many orders of magnitude drop in simulated free CFD lasting more than 30 days following dosing (**Figure 3A**). At the dose range of 1–10 mg per eye, the exposure ranges of lampalizumab in vitreous, aqueous, and retina are above 10 nM (**Figure 2C-E**) during the 16-day study time, and are well above the K_{ss} and K_D value of 11.7 pM (Loyet et al., 2014), suggesting that maximal target-mediated clearance was reached and target-independent linear kinetics is predominant. In fact, **Figure 3B** illustrates that over a large range of ITV dose levels (0.1–50 mg per eye), linear clearance is expected to be predominant. The linear clearance process is governed mainly by the rate of lampalizumab exiting the eye, as evidenced by the similar slopes in the ocular (aqueous, vitreous and retina) concentrations and serum concentrations versus time (**Figure 2B-E**).

Upon exiting the eye, lampalizumab is cleared by two different mechanisms: a linear target-independent clearance mechanism and a target-mediated clearance mechanism. The linear clearance mechanism is characterized by a first-order systemic elimination half-life of 0.8 hours (**Table 2**). This parameter was well estimated (RSE = 1.2%) due to the availability of the serum lampalizumab and CFD data following IV

Downloaded from jpet.aspetjournals.org at ASPET Journals on April 17, 2024

JPET Fast Forward. Published on September 10, 2015 as DOI: 10.1124/jpet.115.227223
This article has not been copyedited and formatted. The final version may differ from this version.

administration. However, the linear clearance mechanism is only a minor pathway for serum lampalizumab clearance, composed of approximately 2–11% of total clearance over the range of 0.1–50 mg lampalizumab per eye (**Figure 4B**). The target-mediated clearance mechanism is responsible for approximatly 90% of lampalizumab clearance in the serum, as a result of lower lampalizumab exposure and higher CFD level in the systemic circulation. The higher serum CFD concentrations, compared with lampalizumab over time in the dosing groups in which both drug and target data were available, suggest that target-mediated clearance is predominant. This is especially true due to the high binding affinity between lampalizumab and CFD (Loyet et al., 2014). The clear indication of target-mediated clearance is also shown by the increase in the total CFD concentrations upon both IV and ITV lampalizumab administration (**Figure 2A-B**). This also confirms the binding of lampalizumab to CFD in vivo as the lampalizumab-CFD complex is expected to clear more slowly than CFD alone, partly because of the larger size of the complex. This is in agreement with the estimated elimination constant parameters of CFD and the lampalizumab-CFD complex, 96 and 4.2 day^{-1}, respectively (**Table 2**). Many studies in the literature also suggested similar mechanisms of slower clearance of complex compared with soluble target (Davda and Hansen, 2010; Hayashi et al., 2007).

Our analysis also revealed that the synthesis rate of CFD in the systemic circulation is 7.8 mg/day (or ~2.6 mg/kg/day for a 3-kg monkey). This is similar to the synthesis rate of CFD in humans. Current literature suggests that rapid synthesis of CFD occurs in the systemic circulation, with an estimated rate of 1.33 mg/kg/day in humans (with a typical body weight of 75 kg) (Pascual et al., 1988). Despite the rapid synthesis of CFD, our simulation studies in the cynomolgus monkey model suggested that only a relatively small amount enters the eye. The cumulative ocular influx of CFD remains less than 0.1 molar fraction of total dose at up to 30 days following ITV administration (**Figure 6**). In a TMDD model in humans, the composite influx rate of CFD into the ocular compartment estimated from the study model was 0.32 µg/ml/day (Le et al., 2015). This accounts for less than 1% of the systemic production rate of 1.33 mg/kg/day.

Downloaded from jpet.aspetjournals.org at ASPET Journals on April 17, 2024

JPET Fast Forward. Published on September 10, 2015 as DOI: 10.1124/jpet.115.227223
This article has not been copyedited and formatted. The final version may differ from this version.

In summary, our model-based PK/PD analysis of lampalizumab in cynomolgus monkeys represents the first analysis to mechanistically examine the interplay between ocular and systemic PK of an antibody in ophthalmology drug development. This study shows that lampalizumab distributes rapidly across the ocular tissues upon ITV administration. Lampalizumab PK exhibits flip-flop kinetics, with slow ocular elimination and rapid systemic elimination. Our analysis also suggests that linear clearance mechanism is predominant in the ocular environment as a result of excess lampalizumab compared to CFD concentration, whereas a target-mediated clearance mechanism is predominant in the systemic circulation due to the low systemic exposure of lampalizumab following ITV administration in the face of high CFD levels resulting from high synthesis. Intravitreal administration of lampalizumab enables high local lampalizumab concentration at site of action while minimizing systemic lampalizumab exposure to ensure patient safety. Near-complete target occupancy is maintained over more than 1 month in the vitreous within the tested dose range, while transient target inhibition is observed in the systemic circulation following lampalizumab ITV administration, with PK profiles favorable for ocular efficacy and systemic safety. The systemic synthesis rate of CFD is rapid, and consistent with values in humans, but ocular influx of factor D into the eye is minimal compared to total ITV drug dose and expected to have no impact on dosing strategy. This study also demonstrated how the ocular microenvironment differs substantially from the systemic circulation regarding the synthesis and turnover rates of the therapeutic target, CFD. The ocular PK/PD parameters from our model may be helpful in predicting human ocular PK and PD for lampalizumab as it is often not possible to sample human ocular tissues.

Downloaded from jpet.aspetjournals.org at ASPET Journals on April 17, 2024

JPET Fast Forward. Published on September 10, 2015 as DOI: 10.1124/jpet.115.227223
This article has not been copyedited and formatted. The final version may differ from this version.

Acknowledgments

Support for third-party writing assistance for this manuscript, furnished by Emma A. Platt, PharmD, of Envision Scientific Solutions, was provided by Genentech, Inc.

Downloaded from jpet.aspetjournals.org at ASPET Journals on April 17, 2024

JPET Fast Forward. Published on September 10, 2015 as DOI: 10.1124/jpet.115.227223
This article has not been copyedited and formatted. The final version may differ from this version.

Authorship Contributions

Participated in research design: van Lookeren Campagne, Damico-Beyer

Conducted in vitro, in vivo, or in silico experiments: Le, Gibiansky, Good, Davancaze, Loyet, Morimoto

Contributed new reagents or analytic tools: Le, Gibiansky, Good, Davancaze, Loyet, Morimoto

Performed data analysis: Le, Gibiansky

Wrote or contributed to the writing of the manuscript: Le, Gibiansky, Good, Davancaze, van Lookeren Campagne, Loyet, Morimoto, Jin, Damico-Beyer, Hanley

Downloaded from jpet.aspetjournals.org at ASPET Journals on April 17, 2024

JPET Fast Forward. Published on September 10, 2015 as DOI: 10.1124/jpet.115.227223
This article has not been copyedited and formatted. The final version may differ from this version.

References

Agoram BM, Martin SW and van der Graaf PH (2007) The role of mechanism-based pharmacokinetic-pharmacodynamic (PK-PD) modelling in translational research of biologics. *Drug Discov Today* **12**: 1018-1024.

Anderson DH, Radeke MJ, Gallo NB, Chapin EA, Johnson PT, Curletti CR, Hancox LS, Hu J, Ebright JN, Malek G, Hauser MA, Rickman CB, Bok D, Hageman GS and Johnson LV (2010) The pivotal role of the complement system in aging and age-related macular degeneration: hypothesis re-visited. *Prog Retin Eye Res* **29**: 95-112.

Barnum SR, Niemann MA, Kearney JF and Volanakis JE (1984) Quantitation of complement factor D in human serum by a solid-phase radioimmunoassay. *J Immunol Methods* **67**: 303-309.

Davda JP and Hansen RJ (2010) Properties of a general PK/PD model of antibody-ligand interactions for therapeutic antibodies that bind to soluble endogenous targets. *MAbs* **2**: 576-588.

de Jong PT (2006) Age-related macular degeneration. *N Engl J Med* **355**: 1474-1485.

Deng R, Iyer S, Theil FP, Mortensen DL, Fielder PJ and Prabhu S (2011) Projecting human pharmacokinetics of therapeutic antibodies from nonclinical data: what have we learned? *MAbs* **3**: 61-66.

Do DV, Pieramici DJ, van Lookeren Campagne M, Beres T, Friesenhahn M, Zhang Y and Strauss EC (2014) A phase ia dose-escalation study of the anti-factor D monoclonal antibody fragment FCFD4514S in patients with geographic atrophy. *Retina* **34**: 313-320.

Fritsche LG, Chen W, Schu M, Yaspan BL, Yu Y, Thorleifsson G, Zack DJ, Arakawa S, Cipriani V, Ripke S, Igo RP, Jr., Buitendijk GH, Sim X, Weeks DE, Guymer RH, Merriam JE, Francis PJ, Hannum G, Agarwal A, Armbrecht AM, Audo I, Aung T, Barile GR, Benchaboune M, Bird AC, Bishop PN, Branham KE, Brooks M, Brucker AJ, Cade WH, Cain MS, Campochiaro PA, Chan CC, Cheng CY, Chew EY, Chin KA, Chowers I, Clayton DG, Cojocaru R, Conley YP, Cornes BK, Daly MJ, Dhillon B, Edwards AO, Evangelou E, Fagerness J, Ferreyra HA, Friedman JS, Geirsdottir A,

Downloaded from jpet.aspetjournals.org at ASPET Journals on April 17, 2024

JPET Fast Forward. Published on September 10, 2015 as DOI: 10.1124/jpet.115.227223
This article has not been copyedited and formatted. The final version may differ from this version.

George RJ, Gieger C, Gupta N, Hagstrom SA, Harding SP, Haritoglou C, Heckenlively JR, Holz FG, Hughes G, Ioannidis JP, Ishibashi T, Joseph P, Jun G, Kamatani Y, Katsanis N, C NK, Khan JC, Kim IK, Kiyohara Y, Klein BE, Klein R, Kovach JL, Kozak I, Lee CJ, Lee KE, Lichtner P, Lotery AJ, Meitinger T, Mitchell P, Mohand-Said S, Moore AT, Morgan DJ, Morrison MA, Myers CE, Naj AC, Nakamura Y, Okada Y, Orlin A, Ortube MC, Othman MI, Pappas C, Park KH, Pauer GJ, Peachey NS, Poch O, Priya RR, Reynolds R, Richardson AJ, Ripp R, Rudolph G, Ryu E, Sahel JA, Schaumberg DA, Scholl HP, Schwartz SG, Scott WK, Shahid H, Sigurdsson H, Silvestri G, Sivakumaran TA, Smith RT, Sobrin L, Souied EH, Stambolian DE, Stefansson H, Sturgill-Short GM, Takahashi A, Tosakulwong N, Truitt BJ, Tsironi EE, Uitterlinden AG, van Duijn CM, Vijaya L, Vingerling JR, Vithana EN, Webster AR, Wichmann HE, Winkler TW, Wong TY, Wright AF, Zelenika D, Zhang M, Zhao L, Zhang K, Klein ML, Hageman GS, Lathrop GM, Stefansson K, Allikmets R, Baird PN, Gorin MB, Wang JJ, Klaver CC, Seddon JM, Pericak-Vance MA, Iyengar SK, Yates JR, Swaroop A, Weber BH, Kubo M, Deangelis MM, Leveillard T, Thorsteinsdottir U, Haines JL, Farrer LA, Heid IM and Abecasis GR (2013) Seven new loci associated with age-related macular degeneration. *Nat Genet* **45**: 433-439, 439e431-432.

Gaudreault J, Fei D, Rusit J, Suboc P and Shiu V (2005) Preclinical pharmacokinetics of Ranibizumab (rhuFabV2) after a single intravitreal administration. *Invest Ophthalmol Vis Sci* **46**: 726-733.

Gibiansky L, Gibiansky E, Kakkar T and Ma P (2008) Approximations of the target-mediated drug disposition model and identifiability of model parameters. *J Pharmacokinet Pharmacodyn* **35**: 573-591.

Girmens JF, Sahel JA and Marazova K (2012) Dry age-related macular degeneration: a currently unmet clinical need. *Intractable Rare Dis Res* **1**: 103-114.

Hayashi N, Tsukamoto Y, Sallas WM and Lowe PJ (2007) A mechanism-based binding model for the population pharmacokinetics and pharmacodynamics of omalizumab. *Br J Clin Pharmacol* **63**: 548-561.

Downloaded from jpet.aspetjournals.org at ASPET Journals on April 17, 2024

JPET Fast Forward. Published on September 10, 2015 as DOI: 10.1124/jpet.115.227223
This article has not been copyedited and formatted. The final version may differ from this version.

Hecker LA, Edwards AO, Ryu E, Tosakulwong N, Baratz KH, Brown WL, Charbel Issa P, Scholl HP, Pollok-Kopp B, Schmid-Kubista KE, Bailey KR and Oppermann M (2010) Genetic control of the alternative pathway of complement in humans and age-related macular degeneration. *Hum Mol Genet* **19**: 209-215.

Holz FG, Strauss EC, Schmitz-Valckenberg S and van Lookeren Campagne M (2014) Geographic atrophy: clinical features and potential therapeutic approaches. *Ophthalmology* **121**: 1079-1091.

Kang-Mieler JJ, Osswald CR and Mieler WF (2014) Advances in ocular drug delivery: emphasis on the posterior segment. *Expert Opin Drug Deliv* **11**: 1647-1660.

Katschke KJ, Jr., Wu P, Ganesan R, Kelley RF, Mathieu MA, Hass PE, Murray J, Kirchhofer D, Wiesmann C and van Lookeren Campagne M (2012) Inhibiting alternative pathway complement activation by targeting the factor D exosite. *J Biol Chem* **287**: 12886-12892.

Krohne TU, Liu Z, Holz FG and Meyer CH (2012) Intraocular pharmacokinetics of ranibizumab following a single intravitreal injection in humans. *Am J Ophthalmol* **154**: 682-686.e682.

Le KN, Gibiansky L, van Lookeren Campagne M, Good J, Davancaze T, Loyet KM, Morimoto A, Strauss EC and Jin JY (2015) Population Pharmacokinetics and Pharmacodynamics of Lampalizumab Administered Intravitreally to Patients with Geographic Atrophy *CPT: Pharmacometrics & Systems Pharmacology* **In press.**

Loyet KM, Deforge LE, Katschke KJ, Jr., Diehl L, Graham RR, Pao L, Sturgeon L, Lewin-Koh SC, Hollyfield JG and van Lookeren Campagne M (2012) Activation of the alternative complement pathway in vitreous is controlled by genetics in age-related macular degeneration. *Invest Ophthalmol Vis Sci* **53**: 6628-6637.

Loyet KM, Good J, Davancaze T, Sturgeon L, Wang X, Yang J, Le KN, Wong M, Hass PE, Campagne M, Haughney PC, Morimoto A, Damico-Beyer LA and DeForge LE (2014) Complement inhibition in cynomolgus monkeys by anti-factor d antigen-binding fragment for the treatment of an advanced form of dry age-related macular degeneration. *J Pharmacol Exp Ther* **351**: 527-537.

Downloaded from jpet.aspetjournals.org at ASPET Journals on April 17, 2024

JPET Fast Forward. Published on September 10, 2015 as DOI: 10.1124/jpet.115.227223
This article has not been copyedited and formatted. The final version may differ from this version.

Luu KT, Kraynov E, Kuang B, Vicini P and Zhong WZ (2013) Modeling, simulation, and translation framework for the preclinical development of monoclonal antibodies. *AAPS J* **15**: 551-558.

Macugen® (pegaptanib sodium) injection [package insert] Palm Beach Gardens, FL: Eyetech, Inc.; 2011.

Mager DE (2006) Target-mediated drug disposition and dynamics. *Biochem Pharmacol* **72**: 1-10.

Mager DE and Jusko WJ (2001) General pharmacokinetic model for drugs exhibiting target-mediated drug disposition. *J Pharmacokinet Pharmacodyn* **28**: 507-532.

Pascual M, Steiger G, Estreicher J, Macon K, Volanakis JE and Schifferli JA (1988) Metabolism of complement factor D in renal failure. *Kidney Int* **34**: 529-536.

Scholl HP, Charbel Issa P, Walier M, Janzer S, Pollok-Kopp B, Borncke F, Fritsche LG, Chong NV, Fimmers R, Wienker T, Holz FG, Weber BH and Oppermann M (2008) Systemic complement activation in age-related macular degeneration. *PLoS One* **3**: e2593.

Schuck E, Bohnert T, Chakravarty A, Damian-Iordache V, Gibson C, Hsu CP, Heimbach T, Krishnatry AS, Liederer BM, Lin J, Maurer T, Mettetal JT, Mudra DR, Nijsen MJ, Raybon J, Schroeder P, Schuck V, Suryawanshi S, Su Y, Trapa P, Tsai A, Vakilynejad M, Wang S and Wong H (2015) Preclinical pharmacokinetic/pharmacodynamic modeling and simulation in the pharmaceutical industry: an IQ Consortium Survey examining the current landscape. *AAPS J* **17**: 462-473.

Stanton CM, Yates JR, den Hollander AI, Seddon JM, Swaroop A, Stambolian D, Fauser S, Hoyng C, Yu Y, Atsuhiro K, Branham K, Othman M, Chen W, Kortvely E, Chalmers K, Hayward C, Moore AT, Dhillon B, Ueffing M and Wright AF (2011) Complement factor D in age-related macular degeneration. *Invest Ophthalmol Vis Sci* **52**: 8828-8834.

Struble C, Howard S and Relph J (2014) Comparison of ocular tissue weights (volumes) and tissue collection techniques in commonly used preclinical animal species. Presented at The European Association for Vision and Eye Research (EVER). October 1-4, 2014. Nice, France.

Downloaded from jpet.aspetjournals.org at ASPET Journals on April 17, 2024

JPET Fast Forward. Published on September 10, 2015 as DOI: 10.1124/jpet.115.227223
This article has not been copyedited and formatted. The final version may differ from this version.

Sunness JS, Rubin GS, Applegate CA, Bressler NM, Marsh MJ, Hawkins BS and Haselwood D (1997) Visual function abnormalities and prognosis in eyes with age-related geographic atrophy of the macula and good visual acuity. *Ophthalmology* **104**: 1677-1691.

Van Der Graaf PH and Gabrielsson J (2009) Pharmacokinetic-pharmacodynamic reasoning in drug discovery and early development. *Future Med Chem* **1**: 1371-1374.

van Lookeren Campagne M, LeCouter J, Yaspan BL and Ye W (2014) Mechanisms of age-related macular degeneration and therapeutic opportunities. *J Pathol* **232**: 151-164.

Wong WL, Su X, Li X, Cheung CM, Klein R, Cheng CY and Wong TY (2014) Global prevalence of age-related macular degeneration and disease burden projection for 2020 and 2040: a systematic review and meta-analysis. *Lancet Glob Health* **2**: e106-116.

Xu L, Lu T, Tuomi L, Jumbe N, Lu J, Eppler S, Kuebler P, Damico-Beyer LA and Joshi A (2013) Pharmacokinetics of ranibizumab in patients with neovascular age-related macular degeneration: a population approach. *Invest Ophthalmol Vis Sci* **54**: 1616-1624.

Downloaded from jpet.aspetjournals.org at ASPET Journals on April 17, 2024

JPET Fast Forward. Published on September 10, 2015 as DOI: 10.1124/jpet.115.227223
This article has not been copyedited and formatted. The final version may differ from this version.

Footnotes

Genentech, Inc., South San Francisco, CA, provided support for the study and participated in the study design; conducting the study; and data collection, management, and interpretation.

Reprint requests:

William Hanley

1 DNA Way, 46-3

South San Francisco, CA 94080

Email: Hanley.william@gene.com

Downloaded from jpet.aspetjournals.org at ASPET Journals on April 17, 2024

JPET Fast Forward. Published on September 10, 2015 as DOI: 10.1124/jpet.115.227223
This article has not been copyedited and formatted. The final version may differ from this version.

Figure Legends

Fig. 1. The ocular and systemic TMDD model structure. C_{free}, R_{VITR}, $R_{SER,}$ and R-C denote free lampalizumab, free CFD in vitreous and serum, and lampalizumab-CFD complex, respectively. F1 denotes the bioavailability of ITV dose that enters the vitreous. CFD, complement factor D; ITV, intravitreal; TMDD, target-mediated drug disposition. Refer to Table 2 for the definition of all other parameters.

Fig. 2. Observed (open circles) and model-predicted (solid lines) total lampalizumab (red) and total CFD (blue) over time in serum following IV (A) and ITV (B) administration, and in vitreous humor (C), aqueous humor (D), and retina (E) following ITV administration. CFD, complement factor D; ITV, intravitreal; IV, intravenous.

Fig. 3. Ocular PK: (A) Simulated vitreous concentration time course of total lampalizumab (solid red line), free lampalizumab (dashed black line), total CFD (solid blue line), free CFD (solid green line), and total lampalizumab-CFD complex (dotted magenta line) following ITV administration (1 and 10 mg/eye). Note: the y-axis is on log-scale to accommodate the different drug and target species, and the small differences in the total lampalizumab and free lampalizumab are not apparent. However, the expected changes in free CFD can be seen by the green line. (B) Lampalizumab fraction of total dose that is cleared by linear clearance (red) and target-mediated drug disposition (TMDD) (blue) as a function of ITV dose. The fractions of drug eliminated by target-mediated clearance (TMCL) and linear CL are defined as total drug elimination through binding to CFD, and through first-order drug clearance mechanism, respectively, normalized by total drug elimination. CFD, complement factor D; ITV, intravitreal; PK, pharmacokinetic.

Fig. 4. Systemic PK: (A) Simulated serum concentration time course of total lampalizumab (solid red line), free lampalizumab (dashed black line), total CFD (solid blue line), free CFD (solid green line), and total lampalizumab-CFD complex (dotted magenta line) following ITV administration (1 and 10 mg/eye). (B) Lampalizumab fraction of total dose that is cleared by linear clearance (red) and target-mediated drug disposition (TMDD) (blue) as a function of ITV dose. The fractions of drug eliminated by target-mediated

Downloaded from jpet.aspetjournals.org at ASPET Journals on April 17, 2024

JPET Fast Forward. Published on September 10, 2015 as DOI: 10.1124/jpet.115.227223
This article has not been copyedited and formatted. The final version may differ from this version.

clearance (TMCL) and linear CL are defined as total drug elimination through binding to CFD, and through first-order drug clearance mechanism, respectively, normalized by total drug elimination. CFD, complement factor D; ITV, intravitreal; PK, pharmacokinetic.

Fig. 5. Time course of target occupancy in vitreous humor and serum as a function of time following intravitreal (ITV) dosing. Black curves represent ocular target occupancy, and red curves represent target occupancy in the serum.

Fig. 6. Time course of target (complement factor D) influx into the vitreous humour following intravitreal (ITV) administration.

Downloaded from jpet.aspetjournals.org at ASPET Journals on April 17, 2024

Table 1. Studies included in the population pharmacokinetic analysis

Study	Molecule/ Species	Route/Dose	Number of Animals/Sex	Number of Samples (sample type)	Sample Collection Time Points (hours)	Study Design	Study Duration
08-1021	LPZ/monkey	IV 0.2 mg/animal	3/M	36 serum (PK, PD)	0, 0.083, 0.5, 1, 2, 3, 5, 8, 24, 34, 96, and 168	Single dose	7 d
		IV 2 mg/animal	3/M	36 serum (PK, PD)			7 d
		IV 20 mg/animal	3/M	36 serum (PK, PD)			7 d
		ITV 1 mg/eye (2 mg/animal)	10/M	140 serum (PK, PD), 29 vitreous (PK, PD), 20 aqueous (PK, PD), 20 retina (PK)	**Serum:** 0, 0.75, 2, 6, 10, 24, 34, 48, 96, 120, 154, 192, 288, 384 **Aqueous:** 24, 48, 120, 192, 384 **Vitreous:** 10, 24, 34, 48, 96, 120, 154, 192, 288, 384 **Retina:** 24, 48, 120, 192, 384		16 d
		ITV 10 mg/eye (20 mg/animal)	10/M	140 serum (PK, PD), 29 vitreous (PK, PD), 20 aqueous (PK, PD), 20 retina (PK)			16 d
08-0782	LPZ/monkey	ITV 1 mg/eye	2/F	14 Serum (PK)	0, 2, 10, 24, 72,	Single dose	12 d

Downloaded from jpet.aspetjournals.org at ASPET Journals on April 17, 2024

JPET Fast Forward. Published on September 10, 2015 as DOI: 10.1124/jpet.115.227223
This article has not been copyedited and formatted. The final version may differ from this version.

Study	Molecule/ Species	Route/Dose	Number of Animals/Sex	Number of Samples (sample type)	Sample Collection Time Points (hours)	Study Design	Study Duration
		ITV 3 mg/eye	2/F	14 Serum (PK)	168, and 264		12 d
		ITV 5 mg/eye	2/F	14 Serum (PK)			12 d
		ITV 10 mg/eye	2/F	14 Serum (PK)			12 d
08-0783	LPZ/monkey	ITV 1 mg/eye	5/M, 5/F	41 Serum (PK)	0, 2, 10, 24, 96, 192, 336, 528, 696, and 1008	Single dose	42 d
		ITV 5 mg/eye	5/M, 5/F	41 Serum (PK)			42 d
		ITV 10 mg/eye	5/M, 5/F	41 Serum (PK)			42 d

ITV, intravitreal; IV, intravenous; LPZ, lampalizumab; PD, pharmacodynamics; PK, pharmacokinetic.

Downloaded from jpet.aspetjournals.org at ASPET Journals on April 17, 2024

JPET Fast Forward. Published on September 10, 2015 as DOI: 10.1124/jpet.115.227223
This article has not been copyedited and formatted. The final version may differ from this version.

JPET Fast Forward. Published on September 10, 2015 as DOI: 10.1124/jpet.115.227223
This article has not been copyedited and formatted. The final version may differ from this version.

Table 2. Model parameters

Parameter	Symbol	Unit	Estimate	RSE (%)
Ocular parameters				
Vitreous volume	V_{VITR}	mL	2.2	7.5
Ocular elimination rate of lampalizumab	k_{out}	day^{-1}	0.24	2.1
Ocular elimination rate of complex	k_{outC}	day^{-1}	0.75	17
Ocular elimination rate of target	k_{outT}	day^{-1}	0.30 Fix	
Ocular influx rate of complex	K_{inC}	day^{-1}	0 Fix	
Vitreous-to-aqueous partition coefficient for lampalizumab	λ_{VA}	dimensionless	4.4	12
Vitreous-to-aqueous partition coefficient for CFD	λ_{TVA}	dimensionless	0.47	24
Vitreous-to-retina partition coefficient for lampalizumab	λ_{VR}	dimensionless	7.3	15
Intravitreal dose fraction to vitreous	F1	dimensionless	0.84	1.2
Systemic parameters				
Serum volume	V_{ser}	mL	130	5.8
Systemic elimination rate of lampalizumab	k	day^{-1}	22	6.6
Systemic elimination rate of CFD	k_{deg}	day^{-1}	96	10
Systemic elimination rate of complex	k_{int}	day^{-1}	4.2	5.6
Synthesis rate of CFD in serum	k_{syn}	nmol/mL/day	2.6	12
Serum-to-ocular transfer rate	k_{sv}	day^{-1}	0.00032	22
Central-to-peripheral distribution rate of lampalizumab	k_{12}	day^{-1}	3.4	12
Peripheral-to-central distribution rate of lampalizumab	k_{21}	day^{-1}	1.8	8.2
Distribution rate of CFD	$k_{t12}=k_{t21}$	day^{-1}	24	54

CFD, complement factor D; RSE, relative standard error.

Downloaded from jpet.aspetjournals.org at ASPET Journals on April 17, 2024

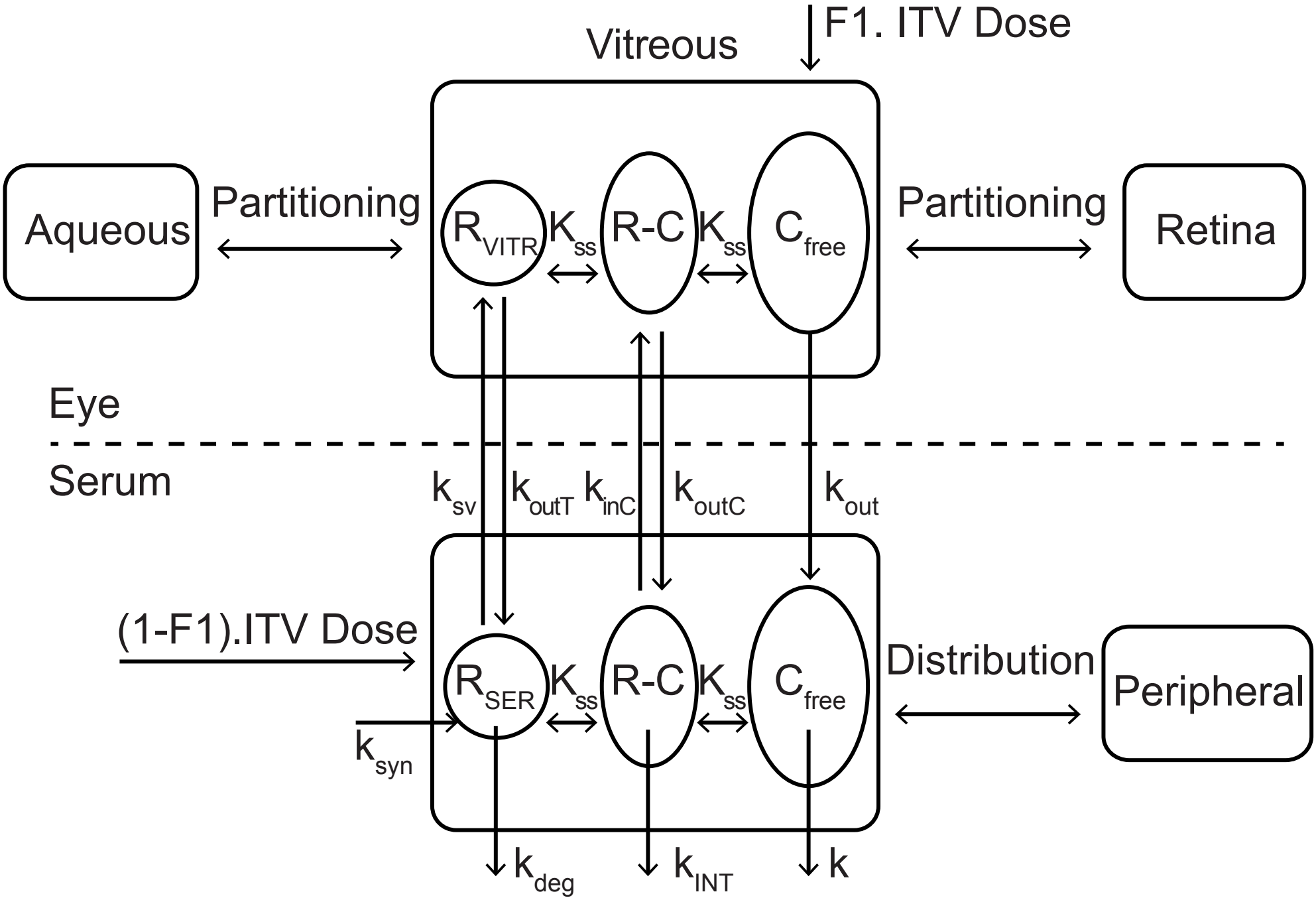
Vitreous
F1. ITV Dose
Aqueous
Partitioning
R_{VITR}
K_{ss}
R-C
K_{ss}
C_{free}
Partitioning
Retina
Eye
Serum
k_{sv}
k_{outT}
k_{inC}
k_{outC}
k_{out}
(1-F1).ITV Dose
R_{SER}
K_{ss}
R-C
K_{ss}
C_{free}
Distribution
Peripheral
k_{syn}
k_{deg}
k_{INT}
k

Figure 1

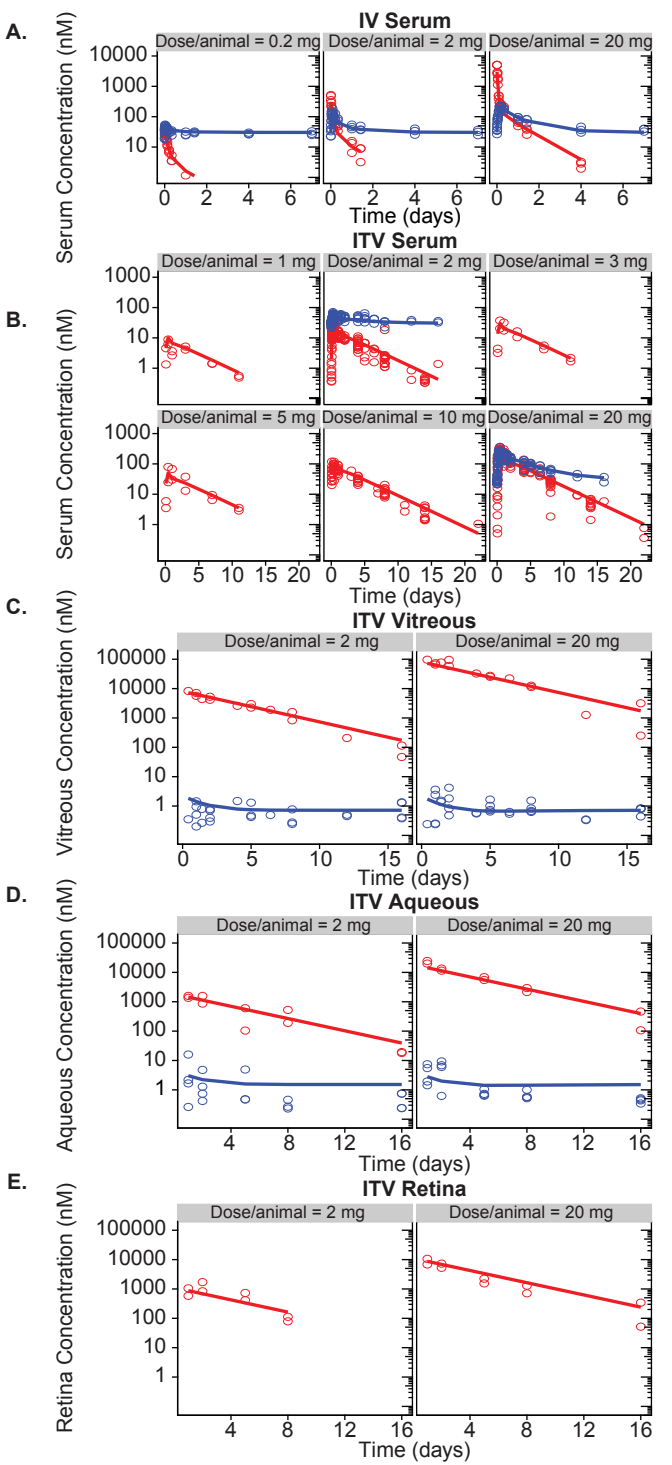
A.
IV Serum
Dose/animal = 0.2 mg
Dose/animal = 2 mg
Dose/animal = 20 mg
Serum Concentration (nM)
10000
1000
100
10
0
2
4
6
Time (days)
B.
ITV Serum
Dose/animal = 1 mg
Dose/animal = 2 mg
Dose/animal = 3 mg
Dose/animal = 5 mg
Dose/animal = 10 mg
Dose/animal = 20 mg
Serum Concentration (nM)
1000
100
10
1
0
5
10
15
20
Time (days)
C.
ITV Vitreous
Dose/animal = 2 mg
Dose/animal = 20 mg
Vitreous Concentration (nM)
100000
10000
1000
100
10
1
0
5
10
15
Time (days)
D.
ITV Aqueous
Dose/animal = 2 mg
Dose/animal = 20 mg
Aqueous Concentration (nM)
100000
10000
1000
100
10
1
4
8
12
16
Time (days)
E.
ITV Retina
Dose/animal = 2 mg
Dose/animal = 20 mg
Retina Concentration (nM)
100000
10000
1000
100
10
1
4
8
12
16
Time (days)

Figure 2

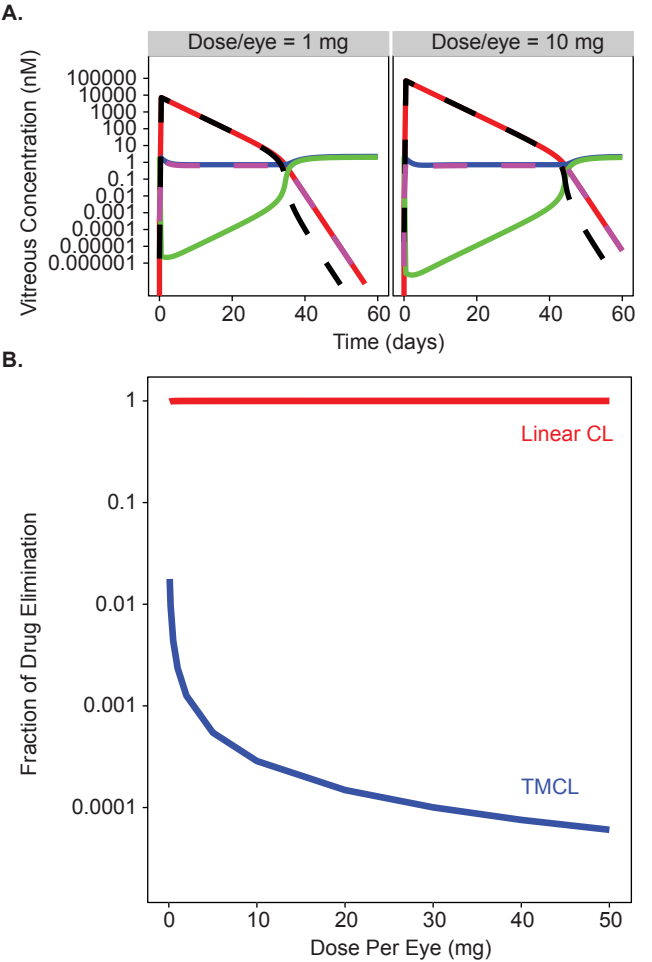
A.
Dose/eye = 1 mg
Dose/eye = 10 mg
Vitreous Concentration (nM)
100000
10000
1000
100
10
1
0.1
0.01
0.001
0.0001
0.00001
0.000001
0
20
40
60
Time (days)
B.
Fraction of Drug Elimination
1
0.1
0.01
0.001
0.0001
Linear CL
TMCL
0
10
20
30
40
50
Dose Per Eye (mg)

Figure 3

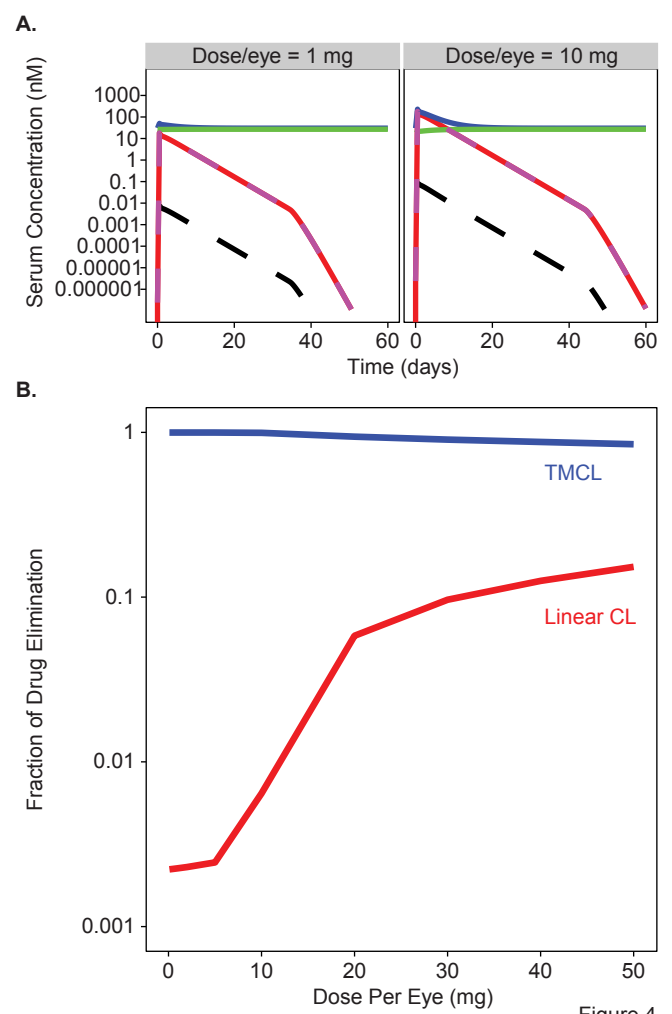
A.
Dose/eye = 1 mg
Dose/eye = 10 mg
Serum Concentration (nM)
1000
100
10
1
0.1
0.01
0.001
0.0001
0.00001
0.000001
0
20
40
60
Time (days)
B.
Fraction of Drug Elimination
1
0.1
0.01
0.001
TMCL
Linear CL
0
10
20
30
40
50
Dose Per Eye (mg)

Figure 4

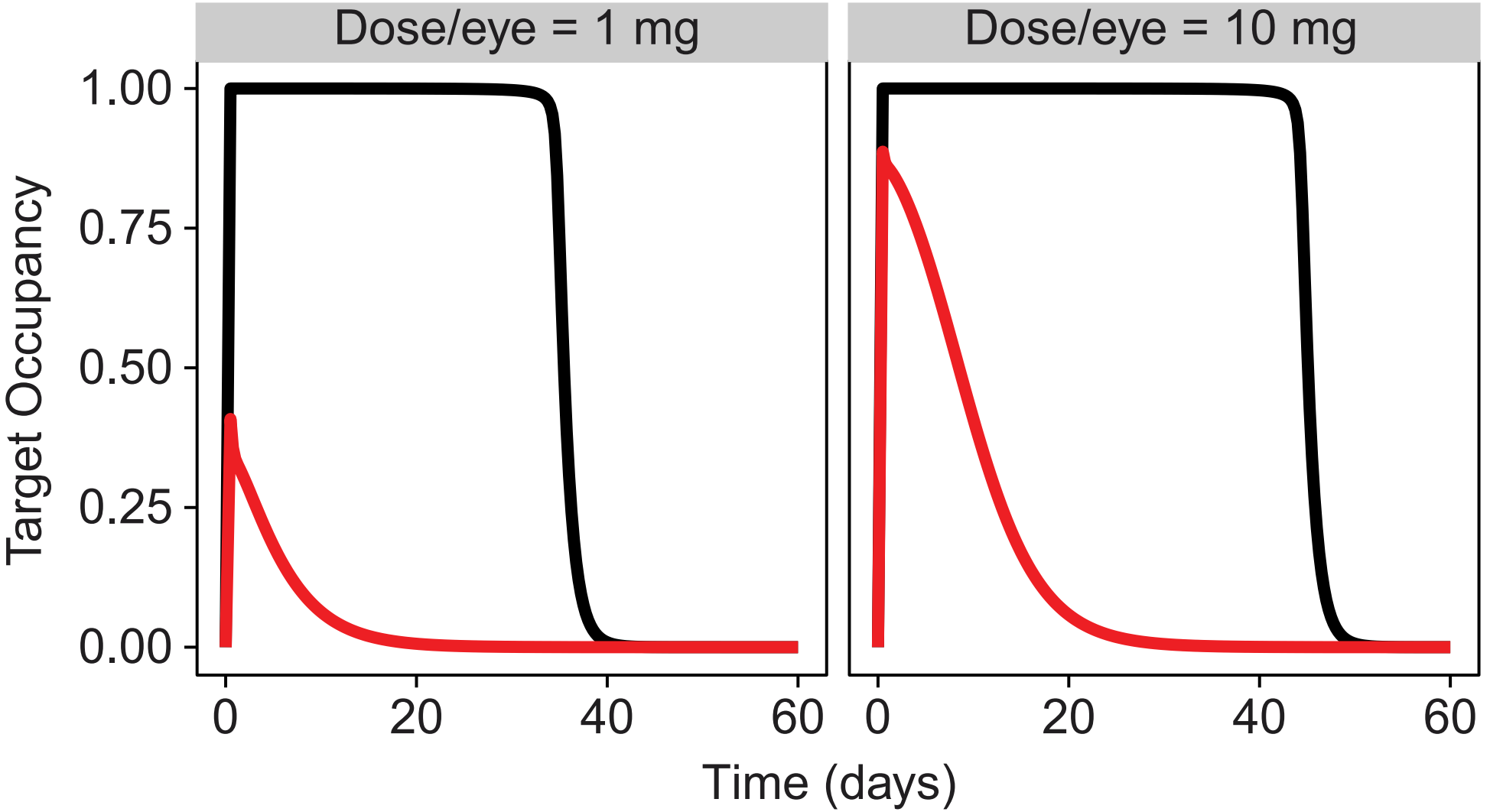
Dose/eye = 1 mg
Dose/eye = 10 mg
Target Occupancy
1.00
0.75
0.50
0.25
0.00
0
20
40
60
Time (days)

Figure 5

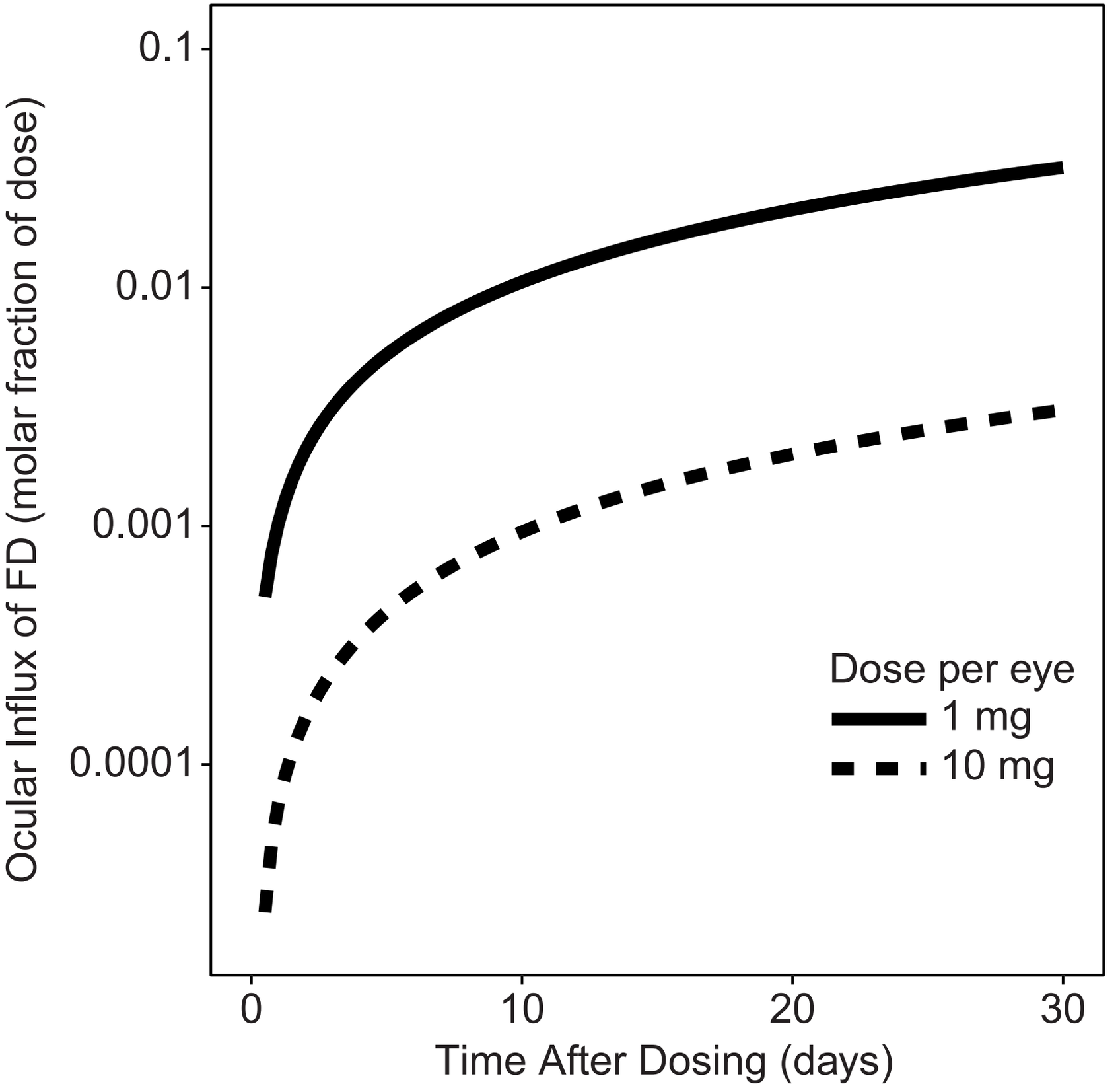
0.1
0.01
0.001
0.0001
Ocular Influx of FD (molar fraction of dose)
0
10
20
30
Time After Dosing (days)
Dose per eye
1 mg
10 mg

Figure 6